Design of secondary optics for IRED in active night vision systems

Di Xin,[1,2] Hua Liu,[1,*] Lei Jing,[1] Yao Wang,[1] Wenbin Xu,[1] and Zhenwu Lu[1]

[1]*Opto-electonics Technology Center, Changchun Institute of Optics, Fine Mechanics and Physics,Chinese Academy of Sciences, Changchun, Jilin 130033, China*

[2]*University of Chinese Academy of Sciences, Beijing 100049, China*

**liuhua_rain@yahoo.com.cn*

Abstract: An effective optical design method is proposed to solve the problem of adjustable view angle for infrared illuminator in active night vision systems. A novel total internal reflection (TIR) lens with three segments of the side surface is designed as the secondary optics of infrared emitting diode (IRED). It can provide three modes with different view angles to achieve a complete coverage of the monitored area. As an example, a novel TIR lens is designed for SONY FCB-EX 480CP camera. Optical performance of the novel TIR lens is investigated by both numerical simulation and experiments. The results demonstrate that it can meet the requirements of different irradiation distances quit well with view angles of 7.5°, 22° and 50°. The mean optical efficiency is improved from 62% to 75% and the mean irradiance uniformity is improved from 65% to 85% compared with the traditional structure.

OCIS codes: (220.4298) Nonimaging optics; (080.2740) Geometric optical design.

References and links

1. J. Moisel, "Solid state night vision systems," Proc. SPIE **5663**, 47–54 (2005).
2. R. M. Wu, Z. R. Zheng, H. F. Li, and X. Liu, "Optimization design of irradiance array for LED uniform rectangular illumination," Appl. Opt. **51**(13), 2257–2263 (2012).
3. S. Zhao, K. Wang, F. Chen, D. Wu, and S. Liu, "Lens design of LED searchlight of high brightness and distant spot," J. Opt. Soc. Am. A **28**(5), 815–820 (2011).
4. *Sony,*http://pro.sony.com/bbsccms/assets/files/mkt/indauto/manuals/FCB-EX480C_EX48C_Technical_Manual.pdf.
5. J. Y. Cai, Y. C. Lo, and C. C. Sun, "Optical design of the focal adjustable flashlight based on a power white-LED," Proc. SPIE **8128**, 812806, 812806-5 (2011).
6. J. J. Chen and C. T. Lin, "Freeform surface design for a light-emitting diode–based collimating lens," Opt. Eng. **49**(9), 093001 (2010).
7. K. L. Huang, J. J. Chen, T. Y. Wang, and L. L. Huang, "Free-form lens design for LED indoor illumination," Proc. SPIE **7852**, 78521D, 78521D-8 (2010).
8. F. Zhao, "Practical reflector design and calculation for general illumination," Proc. SPIE **5942**, 59420J, 59420J-9 (2005).

1 Introduction

A powerful infrared illuminator is the basis of active night vision system [1]. With the gradually increasing output optical power, infrared emitting diode (IRED) has been widely used as the light source of IR-illuminator. In many applications, IR-illuminator should have the ability to change its view angle according to the zoom range of the camera. The view angle is defined as the angle when intensity is half of the value at 0° [2]. The view angle of IR-illuminator should always be bigger than that of the camera. Otherwise the flashlight effect will occur. Therefore, it is necessary to design optical components to make the radiation pattern of IREDs meet the requirements of IR-illuminator, which is so called secondary optical design [3].

#176606 - $15.00 USD Received 21 Sep 2012; revised 24 Oct 2012; accepted 31 Oct 2012; published 10 Jan 2013

At present, most of IR-illuminators commercially available adopt traditional lenses as the secondary optics. Nevertheless, this kind of structure has low optical efficiency because part of light energy cannot be collected by the lens. In addition, variation range of view angle is always not big enough compared with that of the camera, such as SONY FCB-EX 480CP which has the view angle range of 2.8° to 48° [4]. Thus the effective irradiation area is narrowed. Furthermore, due to the low design degree of freedom of lens, the irradiance uniformity reduces quickly as the lens being defocused. The number of lenses of this kind of system is usually more than 1, typically 2 or 3. Increasing the number of lenses will enhance the optical performance, but the complexity of the system will also be increased. Therefore, if we adopt a kind of integrated lens through reasonable optical design to replace the traditional lens as the secondary optics, it will not only reduce the complexity of the system, but also improve the optical performance.

As we all know, the traditional total internal reflection (TIR) lens may have higher optical efficiency than the lens or the reflector because of its specific structure [5]. However, the traditional TIR lens can only provide one view angle, so it is not available to design the IR-illuminator with adjustable view angle. In this study, we propose a novel TIR lens with three segments of the side surface instead of a smooth one as the secondary optics of IR-illumonator, focusing on matching the camera in the view angle and improving the irradiance uniformity as well. A polycarbonate (PC) novel TIR lens with an OSRAM SFH 4235 LED as the light source is designed. Optical performance of the novel TIR lens is investigated by both numerical simulations based on Monte Carlo ray tracing method and experiments. Results demonstrate that the novel TIR optical system has higher optical efficiency and better irradiation performance with three different radiation patterns, which can meet the requirements of IR-illuminators well.

2 Design method of novel TIR lens

2.1 The derivation of view angles

As shown in Fig. 1, the infrared irradiation area is divided into three parts: the near field up to D_1, the middle field from D_1 to D_2 and the far field from D_2 to D_3. Therefore, the IR-illuminator must have the ability to provide three different view angles: the wide one α_w for the near field, the middle one α_m for the middle field and the small one α_s for the far field.

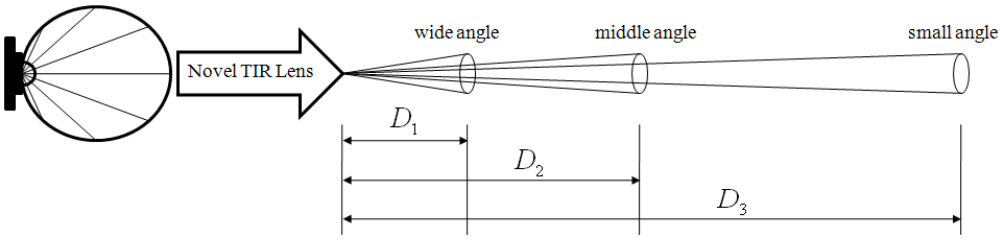

Fig. 1. Radiation distributions of the IR-illuminator.

One of the design targets of the IR-illuminator is to achieve uniform irradiance. The optical power of the IRED is W_t, the target plane is at D_{IR} away from the IRED and the view angle of the IR-illuminator is α. The irradiance on the target plane can be simply calculated as:

$$E = W_t / (\pi D_{IR}^{\ 2} \tan^2(\alpha/2)) \tag{1}$$

The irradiance on the target plane should satisfy:

$$E \geq E_m \tag{2}$$

#176606 - $15.00 USD Received 21 Sep 2012; revised 24 Oct 2012; accepted 31 Oct 2012; published 10 Jan 2013

where E_m is the minimum irradiance of the camera that depends on the type of the used CCD. The relationship between the view angle α and the irradiation distance D_{IR} of the IR-illuminator, (D_{IR}, α), can be obtained using Eq. (1) and (2), and expressed as Eq. (3).

$$W_t / (\pi D_{IR}^2 \tan^2(\alpha/2)) \geq E_m \tag{3}$$

The IR-illuminator should match the camera in the view angle, so the relationship between the view angle β and the monitored distance D_c of the camera, (D_c, β), is deduced as Eq. (4).

$$\frac{h}{2 \times D_c \times \tan(\beta/2)} \geq \eta \tag{4}$$

In Eq. (4), h is the height of the people in the monitored area. The left part represents the ratio of the height of the people to the height of the monitored area. The value range of η is from 0 to 1 and it will be changed with the specific environment and the scale of the monitored area.

Now three view angles of the IR-illuminator can be deduced. The wide view angle α_w should be a little bigger than the biggest view angle of the camera and it can be determined firstly. Then the irradiation distance $D_{IR,w}$ of the IR-illuminator with wide view angle α_w can be obtained through the relationship (D_{IR}, α). After that, we can obtain the view angle β_m of the camera when $D_c = D_{IR,w}$ through (D_c, β). And then the middle view angle α_m of the IR-illuminator can be determined with the requirement of $\alpha_m \geq \beta_m$. Finally the small view angle α_s can be obtained in the same way. These can guarantee that the view angle of the IR-illuminator is always bigger than that of the camera no matter in the near field, middle field or far field.

In this paper, for example, an OSRAM SFH 4235 LED is adpoted as the light source. The optical power is typically 950 mw at 1A. The SONY FCB-EX 480CP camera with the view angle range of 2.8° to 48° is selected. The minimum irradiance E_m is $0.007\, w/m^2$ from experiments. Let $h = 1.75m$ and $\eta = 50\%$ in Eq. (4). Take the equal mark in Eq. (3) and Eq. (4). Following the procedure discussed above, three view angles of the IR-illuminator can be obtained.

As shown in Fig. 2, the biggest view angle of the camera is 48°, so the wide view angle α_w is set to be 50°. From the relationship (D_{IR}, α) the irradiation distance $D_{IR,w}$ of the IR-illuminator with view angle of 50° is 12m. From the relationship (D_c, β), when the monitored distance is 12m, the view angle β_m of the camera is 17°. Then the middle view angle α_m of the IR-illuminator is set to be 22°. The small view angle α_s can be obtained in the same way and its value is 7.5°

#176606 - $15.00 USD Received 21 Sep 2012; revised 24 Oct 2012; accepted 31 Oct 2012; published 10 Jan 2013

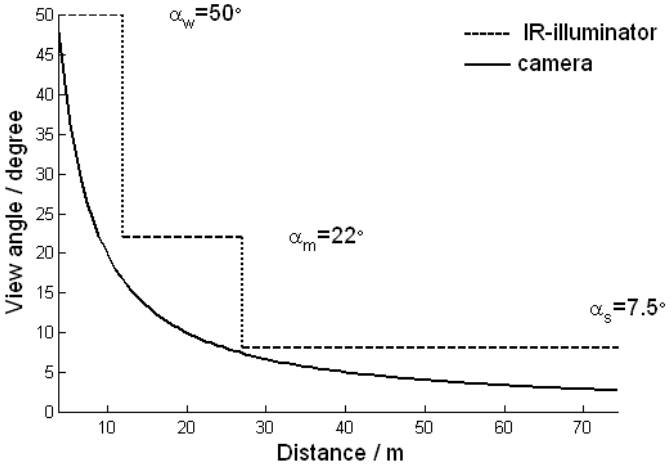

Fig. 2. The view angles versus distance of the IR-illuminator and the camera.

2.2 The calculation of the novel TIR lens

Based on the above discussion, a novel TIR lens with three segments of the side surface can be designed to realize the required view angles when the IRED is at different positions.

Figure 3 shows the two dimensional structure of the novel TIR lens, which is made of PC material and consists of seven optical surfaces: a plane surface AB and a conic surface BC on the rear of the lens, three TIR side surfaces DE, EF and FG, a plane surface in the outer part of the front GH, and a refractive surface in the central part of the front HJ. CD is the base of the lens. θ is a small draft angle for easier mold inset to be pulled out, here, it is 3°. The dashed-line oriented in the z direction is the optical axis of the system. The IRED is denoted by a black rectangle. When the IRED is at P_1, the origin of the coordinates, the view angle of the IR-illuminator is 7.5°. When the IRED is moved to P_2 and P_3, the view angle of the IR-illuminator is 22° and 50° respectively.

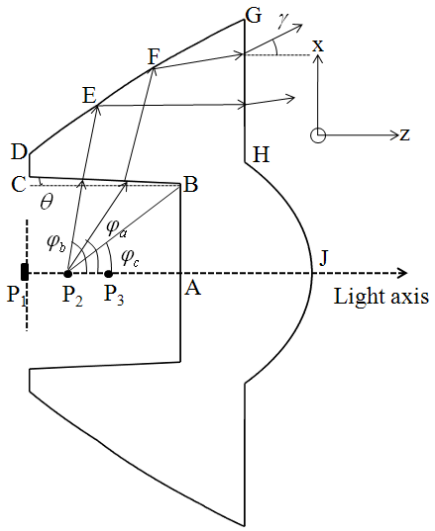

Fig. 3. Two dimensional structure of the proposed TIR lens.

In the design, the IRED is assumed to be an ideal point source.When the IRED is at P_1, the light rays hitting to the refractive surface HJ and the TIR surface DE will exit the lens in a

#176606 - $15.00 USD Received 21 Sep 2012; revised 24 Oct 2012; accepted 31 Oct 2012; published 10 Jan 2013

direction parallel to the optical axis. Thus the two surfaces can be directly calculated. The principle and procedure of surface construction are discussed in detail in reference [6,7]. Once the refractive surface HJ is obtained, the output radiant intensity distribution through the refractive surface when the IRED is moved along light axis to different positions could be calculated using the Snell'Law and the energy conservation law. And then the position P_2 and P_3 can be determined according to the corresponding view angles.

When the IRED is at P_2, the TIR surface EF can be calculated. The IRED is assumed to be an ideal Lambertian source, and so the normalized radiant intensity distribution and the incident cumulative radiant flux can be expressed as:

$$I(\varphi) = \cos\varphi \tag{5}$$

$$\phi_s(\varphi) = \int I(\varphi) dw = \pi \sin^2 \varphi \tag{6}$$

where φ represents the direction of the incident light ray with respect to the light axis and dw is the solid angle. The incident cumulative radiant flux includes two parts: the refracted part $\phi_{refract}(\varphi_r)$ through surface HJ and the TIR part $\phi_{TIR}(\varphi_{TIR})$ through surface EF where $0 \le \varphi_r \le \varphi_c$ and $\varphi_a \le \varphi_{TIR} \le \varphi_b$. As shown in Fig. 3, φ_c is the angle between the line P_{2B} and the light axis. φ_a and φ_b are the angles of the edge rays of the light beam that the TIR surface EF controls. Each of the two parts can be expressed as:

$$\phi_{refract}(\varphi_r) = \pi \sin^2 \varphi_r, \varphi_r \in [0, \varphi_c] \tag{7}$$

$$\phi_{TIR}(\varphi_{TIR}) = \pi(\sin^2 \varphi_b - \sin^2 \varphi_{TIR}), \varphi_{TIR} \in [\varphi_a, \varphi_b] \tag{8}$$

The desired radiant intensity distribution of the IR-illuminator which can achieve the uniform irradiance on the target plane can be expressed as follows [8].

$$I(\gamma) = \frac{I_0}{\cos^3(\gamma)} \tag{9}$$

where γ represents the direction of the output light ray with respect to the light axis. Based on that, the desired total output cumulative radiant flux can be calculated as:

$$\phi_t(\gamma) = I_0 \pi (1/\cos^2 \gamma - 1), \gamma \in \left[0, \frac{\alpha_m}{2}\right] \tag{10}$$

After normalization, $I_0 = 1/(1/\cos^2(\alpha_m/2) - 1)$. Both the refracted part and the TIR part form the energy distribution expressed by Eq. (10). That is:

$$\phi_t(\gamma) = \phi_{refract}(\varphi_r) + \phi_{TIR}(\varphi_{TIR}) \tag{11}$$

Substituting Eq. (7), (8) and (10) into Eq. (11), we can obtain the following equation:

$$\varphi_{TIR} = arc\sin(\sqrt{(\sin^2 \varphi_r + \sin^2 \varphi_b) - I_0(1/\cos^2 \gamma - 1)}) \tag{12}$$

This is an explicit relationship between φ_{TIR} and γ. Using Eq. (12) and following the procedure of surface construction in reference [6,7], the TIR surface EF can be calculated. The TIR surface FG can be calculated in the same way.

#176606 - $15.00 USD Received 21 Sep 2012; revised 24 Oct 2012; accepted 31 Oct 2012; published 10 Jan 2013

3 Simulation and experimental results

With the view angles deduced in section 2.1, a novel TIR lens can be designed according to the preceding method. The optical design parameters are given in Table 1. As shown in Fig. 4, the PC TIR lens was manufactured by injection molding method.

Table 1. Parameters of the Novel TIR Lens

Parameter	Value
Light source	OSRAM SFH 4235 LED
Camera type	SONY FCB-EX 480CP
Lens Material	PC
$\overline{P_1A}$	11.3mm
$\overline{P_1J}$	24mm
Angle between the line P_1B and the light axis	35°
$\overline{CD}$	2mm
$\overline{P_1P_2}$	3.5mm
$\overline{P_1P_3}$	7.8mm

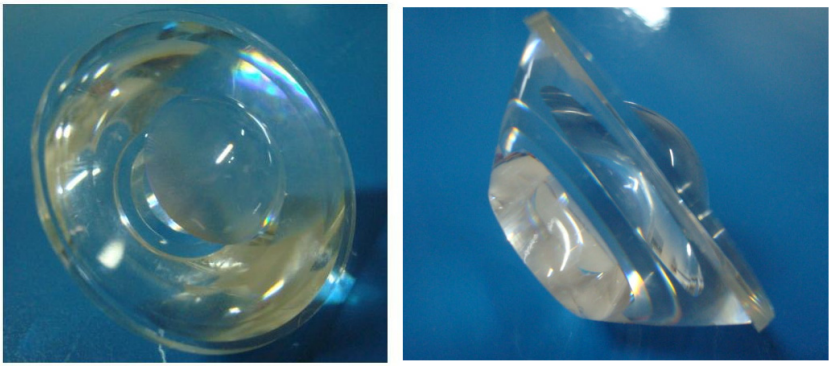

Fig. 4. (a) Front view of and (b) side view of the novel TIR lens.

A TracePro program is employed to trace 1 million light rays emitted from the IRED through the novel TIR lens. Both Fresnel and absorption losses are considered. Figure 5, Fig. 6 and Fig. 7 show the simulation and experimental irradiance maps, and the comparisons between them, respectively. Figure 5 is for the wide view angle of 50°. The target plane in simulation is at 12m away from the IRED; the target plane in experiment is at 1.4m. The optical efficiency is 85%. The irradiance uniformity in the center part is 86%. Here, uniformity is defined as the ratio of the minimum irradiance to the maximum irradiance on the target plane. Figure 6 is for the middle view angle of 22°. The target plane in simulation is at 27m; the target plane in experiment is at 2.9m. The optical efficiency is 77%. The irradiance uniformity in the center part is 87%. Figure 7 is for the small view angle of 7.5°. The target plane in simulation is at 100m; the target plane in experiment is at 3.7m. The optical efficiency is 63%. The irradiance uniformity in the center part is 82%.

Among the three modes, the optical efficiency is the lowest in the mode with small view angle and obvious dim rings exist at the edge of the radiation pattern. These are partly because

#176606 - $15.00 USD Received 21 Sep 2012; revised 24 Oct 2012; accepted 31 Oct 2012; published 10 Jan 2013

EF and FG parts inevitably affect the optical performance of the small-angle mode. Similarly, FG part also affects the optical performance of the middle-angle mode. As we can see from these figures, the size of the irradiance map in experiment is bigger than the size of the irradiance map in simulation and the edge of the parttern is blurred. The central irradiance of experiment is lower than that of simulation. The differences are caused by certain errors in our prototype. In summary, experimental results are close to the simulation results and are also in agreement with the expected performance.

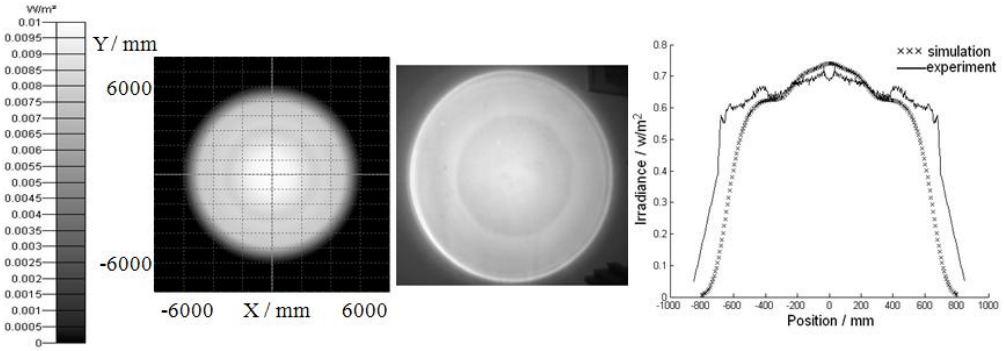

Fig. 5. (a) Simulation irradiance map; (b) experimental irradiance map; (c) comparison of the irradiance distribution between simulation and experiment with view angle of 50°.

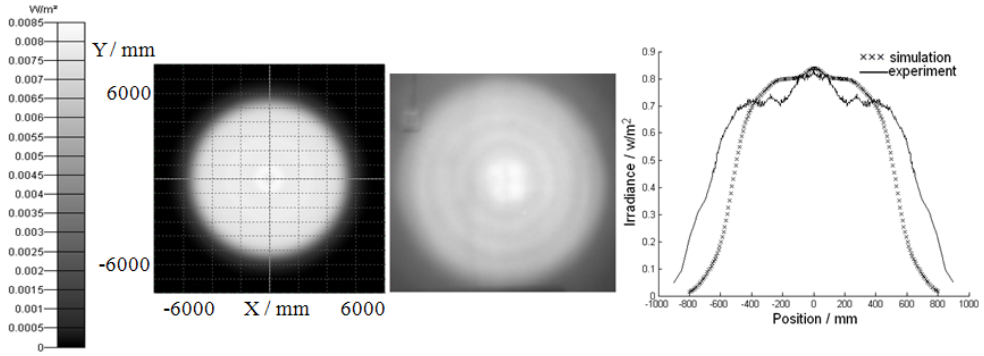

Fig. 6. (a) Simulation irradiance map; (b) experimental irradiance map; (c) comparison of the irradiance distribution between simulation and experiment with view angle of 22°.

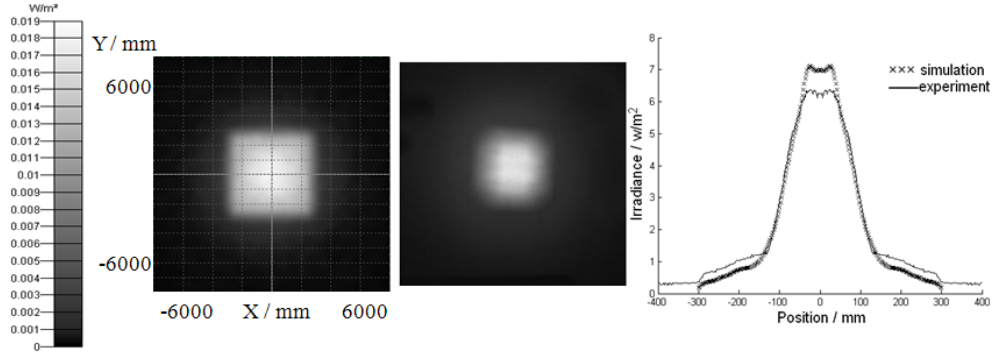

Fig. 7. (a) Simulation irradiance map; (b) experimental irradiance map; (c) comparison of the irradiance distribution between simulation and experiment with view angle of 7.5°.

#176606 - $15.00 USD Received 21 Sep 2012; revised 24 Oct 2012; accepted 31 Oct 2012; published 10 Jan 2013

For comparison, a kind of traditional structure including two lenses, a spherical lens and an aspherical lens, is simulated with the same IRED. The results are shown in Table 2.

Table 2. Comparison between the Novel TIR Lens and Traditional Structure

	View angle	Optical efficiency			Uniformity		
		Wide angle	Middle angle	Small angle	Wide angle	Middle angle	Small angle
Novel TIR lens	7.5° 22° 50°	85%	77%	63%	86%	87%	82%
Traditional structure	7°~40°	70%	68%	47%	50%	54%	90%

We use the mean optical efficiency and mean irradiance uniformity of the three view angles to evaluate the overall performance of the novel TIR lens and the traditional structure. The mean optical efficiency of the novel TIR lens reaches as high as 75%, and it is 62% for the traditional structure. It is shown that the traditional structure has high uniformity of 90% with small view angle. However, when the view angle becomes larger, the uniformity falls quickly to about 50%. The mean value is 65%. The novel TIR lens can keep high uniformity of no less than 80% in the three modes. The mean value is 85%. Furthermore, the maximum view angle of the novel TIR lens is widen from 40° to 50° compared with the traditional structure. Therefore, the whole monitored area can be irradiated.

4 Conclusions

In this study, a novel TIR lens with three segments of the side surface is designed as the secondary optics of the IR-illuminator. By defocusing the novel TIR lens, the IR-illuminator can quickly change the beam size and energy density distribution for various applications. The simulation and experimental results show that the mean uniformity of 85% and mean optical efficiency of 75% with OSRAM SFH 4235 LED can be achieved. The three view angles, 7.5°, 22° and 50°, satisfy a complete coverage of the monitored area. Therefore, it is an effective method to solve the problem of adjustable view angle for IR-illuminator compared with the traditional structure.

Acknowledgments

The authors gratefully acknowledge the financial support from the Innovation Program of Chinese Academy of Sciences (Y10132N110).

#176606 - $15.00 USD Received 21 Sep 2012; revised 24 Oct 2012; accepted 31 Oct 2012; published 10 Jan 2013